DETECTOR RESPONSE FROM THERMAL NEUTRON ACTIVATION OF CONCEALED EXPLOSIVES

ZAFAR ULLAH KORESHI[1*] AND HAMDA KHAN[2]

[1]Faculty of Engineering,
[2]Faculty of Basic and Applied Sciences,
Air University, Islamabad 44000, Pakistan.

[*]Corresponding author: zafar@mail.au.edu.pk

(Received: 18TH Oct. 2016; Accepted: 11th Feb. 2017; Published on-line: 1st Dec. 2017)

ABSTRACT: Explosives concealed in small quatitites (~100 g), buried in landmines, or in baggage, can be detected by characteristic gamma rays produced by neutron activation. However, the detection response can be reduced by attenuation of the signal in the background medium. This paper carries out a Monte Carlo simulation, using MCNP5, to estimate the gamma signal spectrum and intesity degradation at a sodium iodide (NaI) detector from a small sample of trinitrotoluene (TNT) explosive buried in limestone. It is found that the transmission across 25 cm of limestone is ~6% of the 2.2233 MeV hydrogen signal and ~20% of the nitrogen signal. An empirical formula, obtained from MCNP re-runs, is used to estimate the signal strength from TNT, buried at 5-25 cm in limestone, for a californium source (^{252}Cf) emitting 2.31 × 10^7 n/s. It is found that for TNT, mass in the range 0.1-3 kg, the signatures are in the range of 20-2000 s^{-1} from nitrogen and 24-2400 s^{-1} from hydrogen. These estimates can be used to determine the scanning time for an explosives detection system.

ABSTRAK: Bahan letupan tersembunyi pada kuantiti sedikit (~100 g), yang ditanam di kawasan periuk api atau dalam beg, boleh dikesan melalui sinar gama yang dihasilkan melalui pengaktifan neutron. Walau bagaimanapun, tindak balas yang dikesan dapat dikurangkan melalui pelemahan pada signal medium latar belakang. Kertas ini mengguna pakai simulasi Monte Carlo, melalui MCNP5, bagi menganggarkan spektrum signal gama dan pengurangan keamatan pada pengesan Sodium Iodida (NaI) daripada sedikit sampel bahan letupan trinitrotoluene (TNT) yang tertanam di lapangan periuk api. Didapati penghantaran sejauh 25 cm pada batu kapur adalah ~6% pada signal hidrogen 2.2233 MeV dan ~20% pada signal nitrogen. Hasil formula empirik yang dijalankan semula keatas MCNP dan digunakan untuk menganggar kekuatan signal TNT, mendapati 5-25 cm telah tertanam dalam batu kapur, dengan punca kalifornium (^{252}Cf) pada pengeluaran 2.31 x 10^7 n/s. Berat TNT pada skala 0.1-3 kg, adalah sebanyak 20-2000 s^{-1} daripada nitrogen dan 24-2400 s^{-1} daripada hidrogen. Anggaran ini boleh dipakai untuk memperolehi masa imbasan pada sistem pengesan bahan letupan.

KEYWORDS: *explosive detection; landmine detector; thermal neutron activation;Monte Carlo simulation; gamma signature*

1. INTRODUCTION

With an estimated 110 million anti-personnel mines in about 70 countries [1,2], over 26,000 people are maimed or killed every year. It is thus both important and urgent to carry out studies which can lead to useful, efficient, field-portable systems. Chemical

explosives, such as TNT and RDX, contain hydrogen (H), carbon (C), oxygen (O), and nitrogen (N) which can be identified along with their relative atomic compositions enabling identification using nuclear techniques such as Fast Neutron Activation (FNA) and Thermal Neutron Activation (TNA) [3]. Such techniques have been under consideration since the 1960s [4-7] and explosives detection systems (EDS) have been investigated and designed for detection of explosives concealed in vehicles [8], airport baggage [9], air cargo [10], land and sea containers [11, 12], as well as landmines [13-17].

Landmine detection systems [18-28] are based on activation by sources such as ^{252}Cf and use measurements of the 2.2233 MeV and 10.829 MeV gamma rays emitted from the $H(n,\gamma)$ and $N(n,\gamma)$ reactions respectively. Some systems determine the C/O atom fraction with the 6.13 MeV gamma-ray emitted in the $^{16}_{8}O(n,n'\gamma)$reaction. Typical capabilities include the identification of amounts as small as ~400 g of explosive in 10 minutes [22]. Monte Carlo simulation with MCNP [29] and experiments have been carried out [30-34] to optimize the performance of the neutron back-scattering technique (NBS) for a landmine system. Typically, a californium ^{252}Cf source emitting ~10^6 neutrons/s is needed for hand-held detection systems and ~10^7 neutrons/s for robotic detection systems. Studies have also been carried out on the effects of source, moderator, and shielding [35-42]. Another use of results from simulation has been in template-matching algorithms [43, 44] for efficient and fast matching of photon signatures from an interrogated volume.

This work extends the previous works in this area which have been used to simulate neutron and gamma transport in landmine detection systems to estimate the signature quality for potential application in matching algorithms. A Monte Carlo simulation with MCNP5 [29] was carried out to determine the energy spectrum degradation and the reduction in intensity of gamma rays emitted from $H(n,\gamma)$ and $N(n,\gamma)$ reactions in soil consisting of limestone. From these estimates, and using proposed empirical formulae [45] the strength of the gamma-rays reaching the detectors was estimated. Such information can be used to estimate the scanning time for field-portable landmine detection systems.

2. METHODOLOGY AND MODELING

Monte Carlo simulation was used to obtain fluxes and reaction rates in the explosive detection system, using the MCNP5 [29] to model a landmine detection system [45] shown in Fig. 1 with physical data listed in Table 1 and material composition in Table 2.

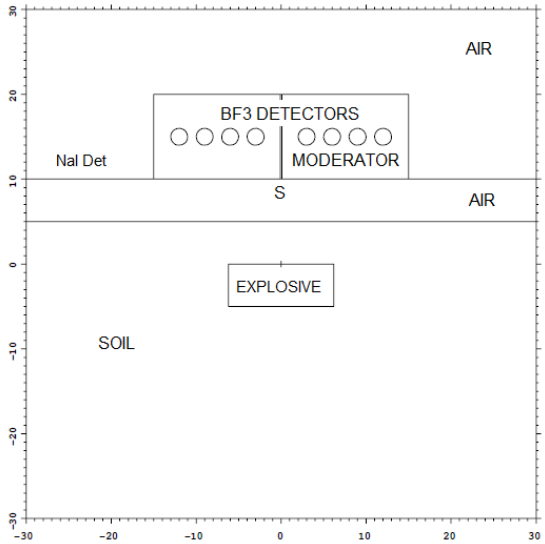

Fig. 1: MCNP model of the landmine explosives detection system (scales in cm).

The neutron and photon fluxes and associated reaction rates from thermal neutron activation of a small (~ 200 g) sample of TNT were obtained. The system consisted of an anisotropic ^{252}Cf source, labeled 'S', placed in a capsule in a moderator with the BF_3 tubes, a sodium iodide (NaI) detector, the soil, and the concealed sample.

The ground considered was limestone ($\rho = 2.71$ g/cm^3 with composition of: C 12%, O 48% and Ca 40%), which is common in many parts of the world.

In a second model, a sphere of radius 25 cm of limestone with a point mono-energetic source at the origin is considered surrounded by sodium iodide detectors, as shown in Fig. 2.

Table 1: Physical data of the model

Source	^{252}Cf
Linear moderator	Borated paraffin wax/water
Explosive	Trinitrotoluene (TNT) $C_6H_2(NO_2)_3CH_3$
Photon detector	Sodium iodide (NaI)
Radial moderator	Borated paraffin wax/water
Neutron detector	BF_3 gas detector
Cavity	Air/water/limestone

Table 2: Composition of materials used (w_i is the mass fraction)

Element and w_i			
Dry Air: $\rho = 0.0012$ g/cm^3			
$^{14}_{7}N$ 0.75519	$^{16}_{8}O$ 0.23179	$^{12}_{6}C$ 0.00014	$^{40}_{18}Ar$ 0.01288
Borated paraffin wax: $\rho = 0.947$ g/cm^3			
$^{1}_{1}H$ 0.14	$^{12}_{6}C$ 0.83	$^{10}_{5}B$ 0.01	$^{11}_{5}B$ 0.02
Limestone: $\rho = 2.71$ g/cm^3			
$^{12}_{6}C$ 0.12	$^{16}_{8}O$ 0.48	$^{40}_{20}Ca$ 0.40	
BF_3: $\rho = 0.002567$ g/cm^3			
$^{10}_{5}B$ 0.143368	$^{11}_{5}B$ 6.568E-3	$^{19}_{9}F$ 0.850064	
TNT: $\rho = 1.654$ g/cm^3			
$^{1}_{1}H$ 0.022189	$^{12}_{6}C$ 0.37016	$^{14}_{7}N$ 0.185004	$^{16}_{8}O$ 0.422648

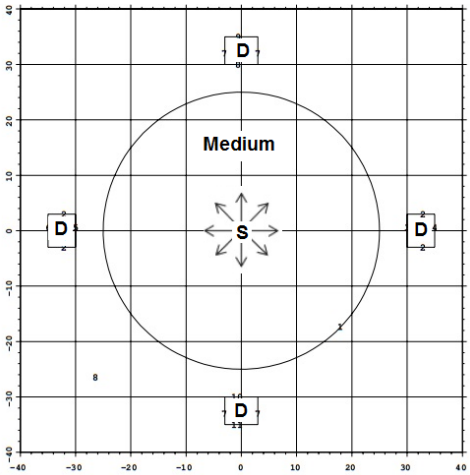

Fig. 2: Gamma transport simulation model (S=source, D=detector, dimensions in *cm*)

A typical photon signal emanating from TNT, illustrating prominent $H(n,\gamma)$ and $N(n,\gamma)$ peaks, buried in limestone, is shown in Fig. 3. It is the transport of these gamma rays which will be considered in the present work.

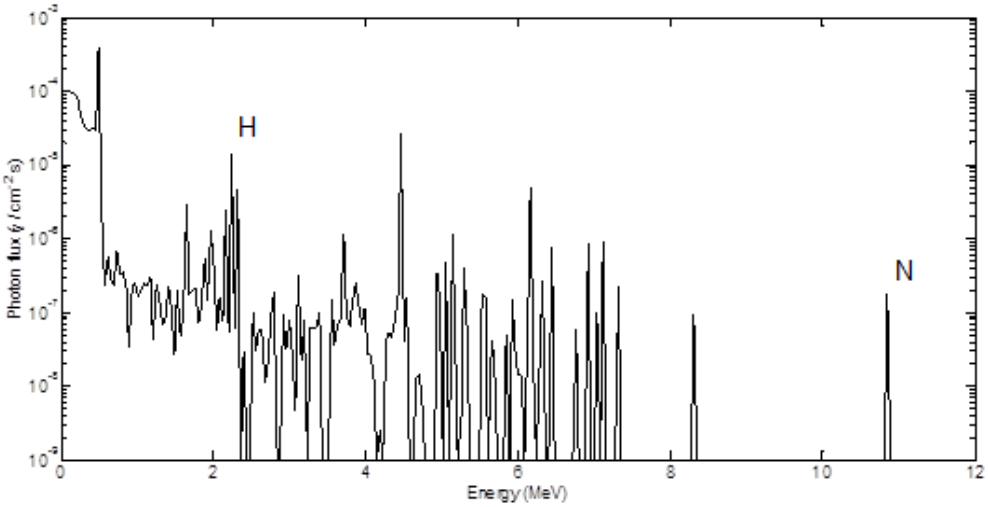

Fig. 3: Typical signature from TNT explosive buried in limestone.

Based on the MCNP results for the model in Fig. 1, a surface fitting of the gamma production in the buried TNT explosive was carried out to obtain an empirical formula of the form $S^i_{(n,\gamma)} = Sf_G f_M f(d,m), i = H,N$ for the gamma production source term $S^i_{(n,\gamma)}$ which is the (n,γ) reaction rate with units atom^{-1} cm^{-3} per source neutron. Here, S is the neutron source strength (n/s), f_G is the geometrical attenuation $d\Omega/4\pi$, f_M is the material attenuation $Be^{-\mu s}$ and $f(d,m)$ is a fitted function containing the burial depth d of explosive mass m. The fitted function is expressed as: $f(d,m) = \sum_{i,j} p_{ij} d^i m^j$, ($i$=1,2,3 and j=1,2,3) with coefficients listed in Table 3.

Table 3: Surface fitted coefficients for the gamma source from TNT explosive buried in a landmine.

Coefficient	$H(n,\gamma)$	$N(n,\gamma)$
p_{00}	1.962×10^{-5}	5.402×10^{-6}
p_{10}	7.851×10^{-6}	1.696×10^{-6}
p_{01}	9.949×10^{-5}	2.157×10^{-5}
p_{20}	-7.131×10^{-7}	-1.592×10^{-7}
p_{11}	-1.632×10^{-6}	-3.140×10^{-7}
p_{02}	-3.614×10^{-5}	-7.878×10^{-6}
p_{30}	1.569×10^{-8}	3.532×10^{-9}
p_{21}	-3.734×10^{-8}	-9.149×10^{-9}
p_{12}	9.013×10^{-7}	1.929×10^{-7}
p_{03}	1.951×10^{-6}	1.275×10^{-7}

2.1 Energy Spectrum Degradation for Photon Transport in Medium

In order to estimate the quality of the transmitted signal, a Monte Carlo simulation is carried out for the gamma signatures from hydrogen and nitrogen shown in Fig. 3. For detection of nitrogen in the signal, the 10.829 MeV gamma ray is considered although its

intensity is ~47% relative to the 5.269 MeV emission, but this is preferred in a counting system due to its high energy.

The total intensity at a detector $I(r)$, located at a distance r from the source, from both un-collided ($I(r)^0$) and collided ($I(r)^s$) rays, is written as a buildup factor $B(r)$ [46] multiplied by the un-collided intensity. Thus

$$B(r) = \frac{I(r)}{I(r)^0} = \frac{I(r)^0 + I(r)^s}{I(r)^0} = 1 + \frac{I(r)^s}{I(r)^0} \tag{1}$$

while the intensity of the un-collided flux when a ray from the source, of intensity $I(0)$, reaches the detector after passing a thickness *t* of the medium is

$$I(r)^0 = \frac{I(0)}{4\pi r^2} e^{-\mu(E_o)t} \tag{2}$$

where μ is the linear attenuation coefficient at source energy E_o. There is a large body of data for point isotropic sources of photons in infinite homogenous media which accounts for Compton-scattered and annihilation photons as well as for fluorescence and bremsstrahlung. A widely used form for the buildup factor is the geometric progress (GP) form:

$$B(E_o, \mu r) = \begin{cases} 1 + \frac{(b-1)(K^{\mu r}-1)}{K-1}, K \neq 1 \\ 1 + (b-1)\mu r, K = 1 \end{cases} \tag{3}$$

where

$$K(\mu r) = c(\mu r)^a + d\frac{\tanh\left(\frac{\mu r}{\xi} - 2\right) - \tanh(-2)}{1 - \tanh((-2)}$$

in which the parameters $a, b, c, d,$ and ξ depend on the gamma ray energy, the attenuating medium and the type of response. These are tabulated for attenuation in air, water, concrete, iron, and lead [46]. For this work, the mass attenuation coefficient ($^{\mu}/_{\rho}$) for limestone is calculated from the weight fractions (*w*) of *C*, *O,* and *Ca* and the elemental coefficients [47] listed in Table 4. From the elemental data, the mass attenuation coefficient of a compound such as limestone is given by

$$^{\mu}/_{\rho} = \sum_i w_i \left(^{\mu}/_{\rho}\right)_i \tag{4}$$

from which the intensity (Eq. 2) can be calculated.

Table 4: Mass attenuation coefficients for photons

i	***w***	$^{\mu}/_{\rho}$ (cm^2/g)		
		2 MeV	10 MeV	15 MeV
carbon	0.12	4.442E-02	1.959E-02	1.698E-02
oxygen	0.48	4.459E-02	2.089E-02	1.866E-02
calcium	0.40	4.524E-02	2.839E-02	2.838E-02

3. RESULTS

The MCNP current tally, scoring the photon current leaving the sphere, is shown in Figs. 4-6 for the total current and un-collided current of photons from hydrogen and neutron using third-order polynomials as fitting functions for 7 MC runs (at R= 2, 5, 10, 15, 20, 25, 30 cm). All simulations were carried out for 400,000 particles and used about 1 minute CPU time on Intel(R) Core(TM) i7-2620M CPU @ 2.70 GHz.

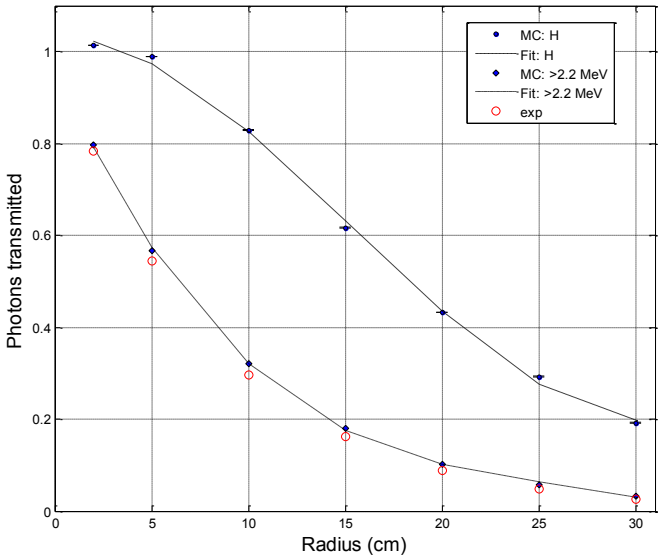

Fig. 4: Photons from hydrogen transmitted versus sphere radius.

Figure 4 shows the total photon transmission and the un-collided (E> 2.2 MeV) photon transmission, the ratios being the build-up $B(r)$ described by Eq. (1). These results can be used to obtain the coefficients in the GP form given by Eq. (3). Further, the excellent match of the MCNP F1 current tally estimates with the simple un-collided exponential attenuation modeled by Eq. (2) is visible in Figs. 4 and 5.

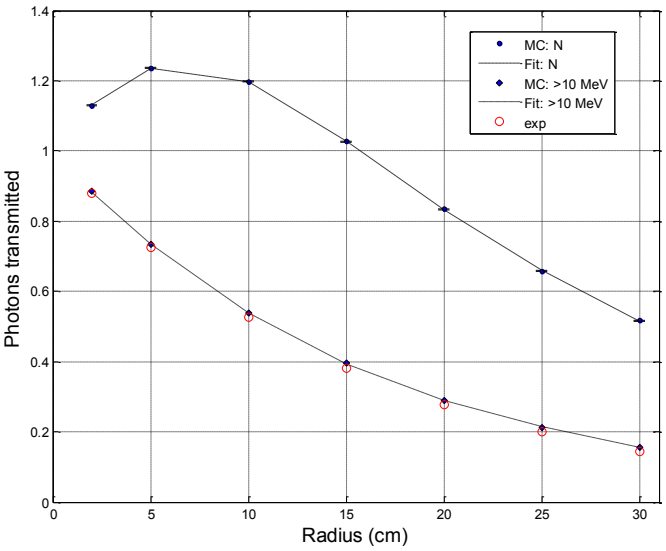

Fig. 5: Photons from nitrogen transmitted as a function of the (limestone) sphere radius.

For a smaller sphere, the number of captures is much lower and consequently the photon creation by bremsstrahlung and fluorescence is also much less. However, these additional photons escape from the sphere and hence the transmitted number exceeds the number of source photons. It is also seen that the 'un-collided' signal (E> 2.22 MeV) decreases exponentially with distance while the total signal falls off almost linearly.

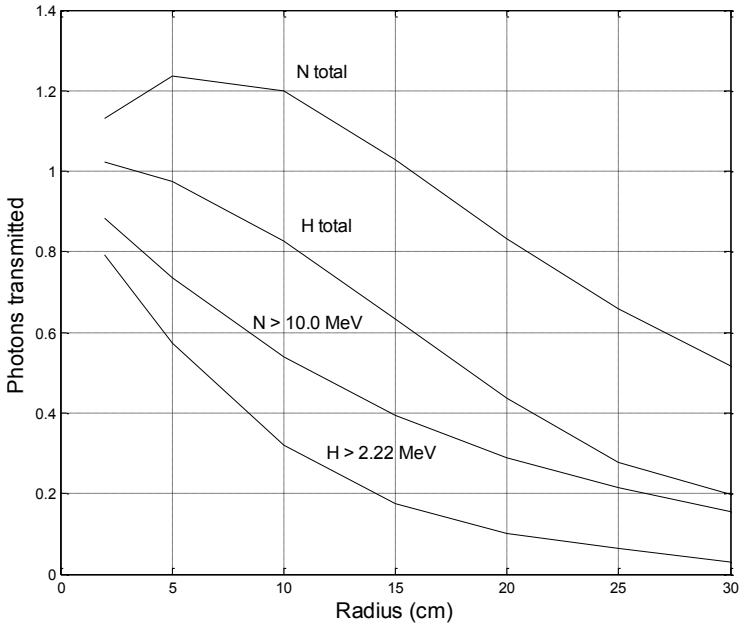

Fig. 6: Photon transmission (2.2233 MeV: *H* and 10.8 MeV: *N*).

Figure 6 shows that the more energetic 10.829 MeV gammas from nitrogen have a much higher transmission across limestone. Thus, while the reaction rate for the radiative capture reaction is much higher for $H(n,\gamma)$ reactions, the transmission balances out the signatures.

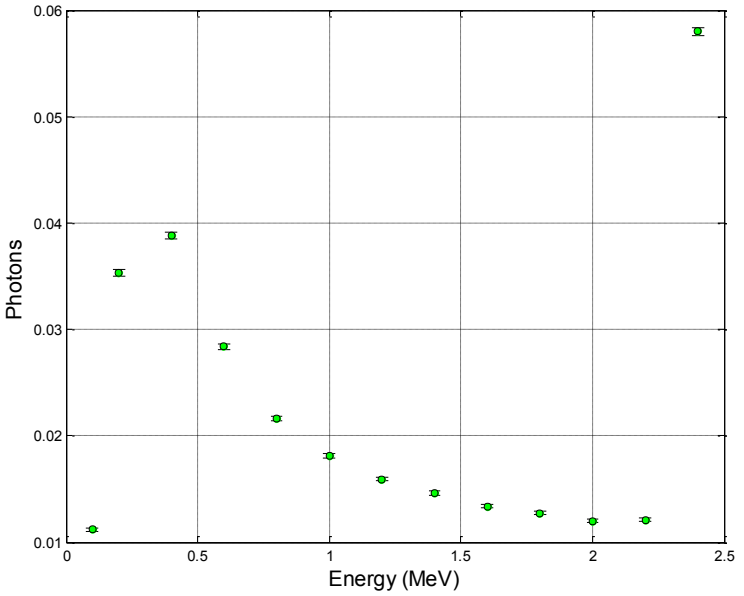

Fig. 7: Energy spectrum of 2.2233 MeV photons leaving the medium.

Figure 7 shows the energy spectrum of the 2.2233 MeV photons leaving the limestone sphere. It is worth noting that only about 5.8% of the photons have source energy (about 8% $E>$ 2 MeV) while about 29.2% of the gammas leave the sphere. The degradation of the spectrum is thus over 90%.

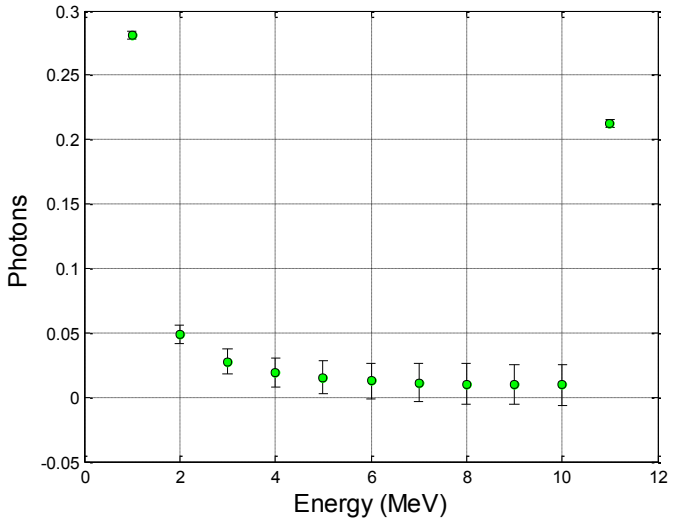

Fig. 8: Energy spectrum of 10.8 MeV photons leaving medium.

Figure 8 shows the energy spectrum of the 10.8 MeV photons leaving the limestone sphere. It is worth noting that only about 21.3% of the photons have source energy. The degradation of the spectrum is thus about 79%.

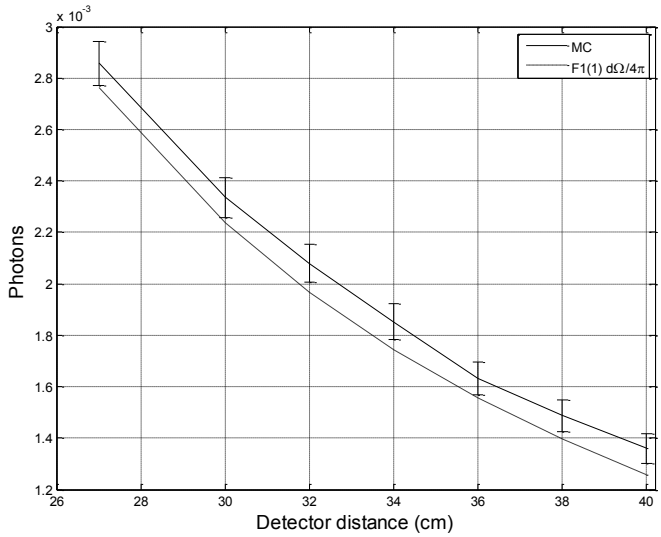

Fig. 9: Photons from 10.8 MeV point source crossing detector; MC results compared with solid angle estimate.

Figure 9 shows the MC results for photons crossing the 3.5 cm radius detector cylinder after passing through a 25 cm radius limestone sphere. Each simulation was carried out for 400,000 particles and took approximately 1.4 minutes. The fraction crossing the limestone sphere was 0.658043 with a relative error of 0.0016.

Now, using the empirical form for the gamma production and a source strength of the order of 10^7 n/s, the total gamma source in the concealed explosive for mass in the range of 0.1 - 3.2 kg at depths 5-25 cm, ranges from 100 – 10,000 photons/s from nitrogen and 400 - 40,000 photons/s from hydrogen [45]. Using results from Figs. 4 and 5, we have seen that only ~6% of the 2.2233 MeV and ~20% of the 10.8 MeV signals leave the ground. It is thus estimated that the hydrogen and nitrogen signatures are down to very low values e.g. 20–2000 s^{-1} from nitrogen and 24–2400 s^{-1} from hydrogen respectively (for the mass range 0.1–3 kg). Thus, for efficient scanning, the scan time must be increased to match the resolution of the hardware.

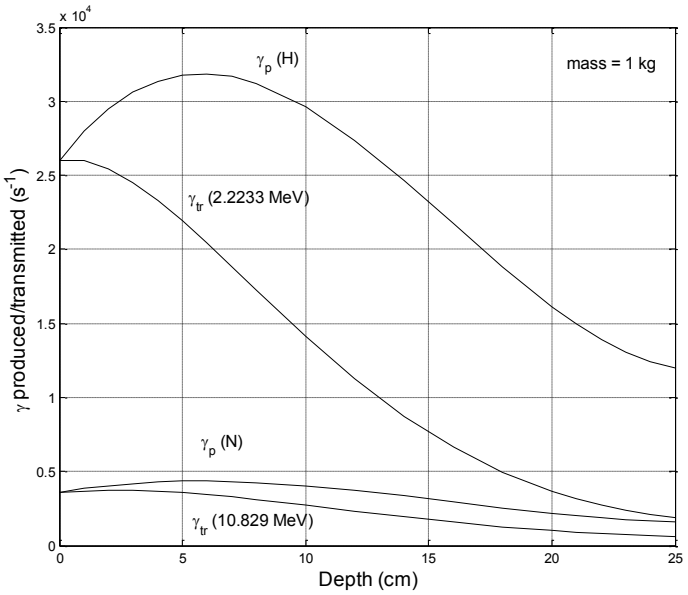

Fig. 10: Gamma production/transmission rate from radiative capture in the explosive.

The gamma production and transmission rates for both *H* and *N* from 1 kg of TNT in limestone are shown in Fig. 10 for a source strength of 2.31 10^7 n/s. This would be an estimate for the 'un-collided' signals leaving the medium. The detector signal would subsequently be obtained by multiplying the above by the solid angle subtended by the detector.

4. CONCLUSIONS

The main conclusions from this Monte Carlo simulation carried out for the landmine detection system based on neutron backscattering are

- The energy spectrum is considerably attenuated and degraded with the depth of concealment in limestone in both hydrogen and nitrogen with only ~6% of the hydrogen signature and ~20% of the nitrogen signature being available for detection when the depth of concealment is 25 cm.
- To effectively detect and characterize a concealed explosive in limestone, the scanning time can be estimated by matching the signature counts with the hardware.

REFERENCES

[1] United Nations, Global Issues, http://www.un.org/en/globalissues/demining/ last accessed 17 September 2016

[2] Walsh NE, Walsh WS. (2003) Rehabilitation of landmine victims – the ultimate challenge, Bulletin of the World Health Organization. 81(9):665-670.

[3] Gozani T. (2004) The role of neutron based inspection techniques in the post 9/11/01 era. Nucl. Instrum. Methods Phys. Res. B. 213:460–463.

[4] Jordan ED. (1964) Detecting hidden explosives using neutron beams Patent No. US 3146349 A, Aug 25, 1964.

[5] Bartko J. (1974) Nuclear techniques for detecting the presence of explosives, Patent No. US 3832545 A Aug 27, 1974. https://www.google.com/patents/US3832545

[6] Ettinger KV, Brondo JH Jr. (1989) Detection of nitrogen in explosives, Patent No. US 4851687 A, Jul 25, 1989. https://www.google.com/patents/US4851687

[7] Grenier G, Coursant RH, Rambaut M. (1992) Apparatus for the detection of substances and in particular explosives by neutron irradiation thereof, Patent No. US 5080856 A, Jan 14, 1992.

[8] Koltick D, Kim Y, McConchie S, Novikov I, Belbot M, Gardner G. (2007) A Neutron Based Vehicle-borne Improvised Explosive Device Detection System. Nucl. Instrum. Methods Phys. Res. B 261:277-280.

[9] Gokhale PP, Hussein EMA. (1997) A ^{252}Cf neutron transmission technique for bulk detection of explosives. Appl Radiat Isot, 48:973-979.

[10] Runkle RC, White TA, Miller EA, Caggiano JA, Collins BA. (2009) Photon and Neutron Interrogation Techniques for Chemical Explosives Detection in Air Cargo: A Critical Review. Nucl Instrum Methods Phys Res A. 603:510-528.

[11] Lehnert AL, Kearfott KJ. (2015) A flag-based algorithm and associated neutron interrogation system for the detection of explosives in sea–land cargo containers. Radiat Phys Chem, 112:13-21.

[12] Heider SA, Dunn WL. (2015) A simulation study of fast neutron interrogation for standoff detection of improvised explosive devices. Radiation Physics and Chemistry. 116:341–344, Proceedings of the 9th International Topical Meeting on Industrial Radiation and Radioisotope Measurement Applications.

[13] Hussein EMA, Waller EJ. (2000) Landmine detection: the problem and the challenge. Appl Radiat Isot, 53:557-563.

[14] Buffler A. (2004) Contraband detection with fast neutrons. Radiation Physics and Chemistry, 71(3-4):853–861.

[15] Kuznetsov AV, Osetrov P, Stancl M (2006). Detection of Improvised Explosives (IE) and Explosive Devices (IED) in Detection and Disposal of Improvised Explosives, H. Schubert and A. Kuznetsov, Springer, Netherlands, 7-25.

[16] Lanza RC. (2007) Neutron Techniques for Detection of Explosives in "Counterterrorist Detection Techniques of Explosives," Yinon, J., Elsevier B.V., Netherlands, 131-155.

[17] Whetstone ZD, Kearfott KJ. (2014) A review of conventional explosives detection using active neutron interrogation. J Radio Nuc Chem, 301:629-639.

[18] Viesti G, Cinausero M, Cufaro-Petroni N, D'Erasmo G, Fabris D, Fioretto E, R, Lunardon M, Lazzizzera I, Nardelli G, Nardulli G, Nebbia G, Palomba M, Pantaleo A, Pappalardo L, Pesente S, Prati P, Prete G, Reito S, Sartori A, Tecchiolli G, Zavatarelli S, Filippini V. (1999) The EXPLODET project: advanced nuclear techniques for humanitarian demining. Nucl Instrum Methods Phys Res A, 422:918-921.

[19] Viesti G, Lunardon M, Nebbia G, Barbui M, Cinausero M, D'Erasmo G, Palomba M, Pantaleo A, Obhođaš J, Valković V. (2006) The detection of landmines by neutron backscattering: Exploring the limits of the technique. Appl Radiat Isot, 64:706-716.

[20] Cinausero M, Lunardon M, Nebbia G, Pesente S, Viesti G, Filippini V. (2004) Development of a thermal neutron sensor for Humanitarian Demining. Appl Radiat Isot, 61:59-66.

[21] Csikai J, Dóczi R, Király B. (2004) Investigations on landmine detection by neutron-based techniques. Appl Radiat Isot, 61:11-20.
[22] Kuznetsov AV, Evsenin AV, Gorshkov IY, Osetrov OI, Vakhtin DN. (2004) Detection of buried explosives using portable neutron sources with nanosecond timing. Appl Radiat Isot, 61:51-57.
[23] Lunardon M, Nebbia G, Pesente S, Viesti G, Barbui M, Cinausero M, D'Erasmo G, Palomba M, Pantaleo A, Filippini A. (2004) Detection of landmines by using 14 MeV neutron tagged beams. Appl Radiat Isot, 61:43-49.
[24] Brooks FD, Drosg M, Buffler A, Allie MS. (2004) Detection of anti-personnel landmines by neutron scattering and attenuation. Appl Radiat Isot, 61:27-34.
[25] Brooks FD and Drosg M. (2005) The HYDAD-D antipersonnel landmine detector. Appl Radiat Isot, 63:565-674.
[26] Takahashi Y, Misawa T, Masuda K, Yoshikawa K, Takamatsu T, Yamauchi K, Yagi T, Pyeon CH, Shiroya S. (2010) Development of landmine detection system based on the measurement of radiation from landmines. Appl Radiat Isot, 68:2327-2334.
[27] Takahashi Y, Misawa T, Pyeon CH, Shiroya S, Yoshikawa K. (2011) Landmine detection method combined with backscattering neutrons and capture γ-rays from hydrogen. Appl Radiat Isot, 69:1027-1032.
[28] Bergaoui A, Reguigui N, Gary CK, Brown C, Cremer JT, Vainionpaa JH, Piestrup MA. (2014) Monte Carlo simulation of explosive detection system based on a Deuterium–Deuterium (D–D) neutron generator. Appl Radiat Isot, 94:118-124.
[29] Girard SM, Shinn JB (2003) MCNP – A General Monte Carlo N-Particle Transport Code, Version 5, LA-UR-03-1987, Los Alamos National Laboratory, Los Alamos, NM.
[30] Maučec M and de Meijer RJ (2002) Monte Carlo simulations as a feasibility tool for non-metallic land-mine detection by thermal-neutron backscattering. Appl Radiat Isot, 56:837-846.
[31] Maučec M, Rigollet, C.(2004) Monte Carlo simulations to advance characterisation of landmines by pulsed fast/thermal neutron analysis. Appl Radiat Isot, 61:35-42.
[32] Perot B, Carasco C, Bernard S, Mariani A, Szabo JL, Sannie G, Valkovic V, Sudac D, Viesti G, Lunardon M., Botosso C, Nebbia G, Pesente S, Moretto S, Zenoni A, Donzella A, Moszynski M, Gierlik M, Klamra W, Tourneur PL, Lhuissier M, Colonna A, Tintori C, Peerani P, Sequeira V, Salvato M. (2008) Measurement of 14 MeV neutron-induced prompt gamma-ray spectra from 15 elements found in cargo containers. Appl Radiat Isot, 66:421-434.
[33] Uchai W, Changkian S, Zhu L, Sun H. (2008) Experiment on the Performance of the Neutron based Explosives Detection System using 252Cf. Suranaree J. Sci. Tech. 15:139-147.
[34] Elsheikh N, Viesti G, ElAgib I, Habbani F. (2012) On the use of a (252Cf–3He) assembly for landmine detection by the neutron back-scattering method. Appl Radiat Isot, 70:643-649.
[35] Baysoy DY, Subasi M. (2013) Numerical Evaluation of a Landmine Detection System based on the Neutron Back Scattering Technique. Academic Journals, 8:1424-1430.
[36] Hernández-Adame PL, Castro DM, Rodriguez-Ibarra JL, Luevano MAS, Carrillo HRV. (2016) Design of an explosive detection system using Monte Carlo method. Appl Radiat Isot, Available online 13 April 2016
[37] http://www.sciencedirect.com/science/article/pii/S0969804316301324
[38] ElAgib I, Elsheikh N, AlSewaidan H, Habbani F. (2009) Monte-Carlo simulations of elastically backscattered neutrons from hidden explosives using three different neutron sources. Appl Radiat Isot, 67: 39-45.
[39] Castro VA, Cavalieri TA, Siqueira PTD, Fedorenko GG, Coelho PRP, Filho TM. (2011) MCNP Simulation to Study the BF3 Detection Efficiency, 2011 International Nuclear Atlantic Conference – INAC 2011 Belo Horizonte, M. G., Brazil, October 24-28, 2011 Associação Brasileira De Energia Nuclear- Aben ISBN:978-85-99141-04-5.
[40] Miri-Hakimabad H, Vejdani-Noghreiyan A, Panjeh H. (2008) Improving the moderator geometry of an anti-personnel landmine detection system. Appl Radiat Isot, 66:606-611.

[41] Metwally WA. (2015) Multi-parameter optimization of a neutron backscattering landmine detection system, Appl Radiat Isot, 105: 290-293.
[42] Koreshi Z, Khan H. (2016) Optimization of Moderator Design for Explosive Detection by Thermal Neutron Activation (TNA) using a Genetic Algorithm, J Nuc Eng Rad Sci, 2: 031018.
[43] Ochbelagh RD, Miri-Hakimabad H, Izadi-Najafabadi R. (2007) The effect of source shield on landmine detection. Iran J Radiat Res, 4:183-186.
[44] Loschke KW, Dunn WI. (2010) Detection of chemical explosives using multiple photon signatures. Appl Radiat Isot, 68:884-887.
[45] Brewer RL, Dunn WL, Heider S, Matthew C, Yang X. (2012) The signature-based radiation-scanning approach to standoff detection of improvised explosive devices, Appl Radiat Isot, 70:1181-1185.
[46] Khan H, Koreshi Z, Yaqub M (2017) Design sensitivity studies of a landmine explosive detection system based on neutron backscattering using Monte Carlo simulation, Nucl Tech Rad Prot, XXXII:37-43.
[47] Cacuci DG. (2000) Nuclear Engineering Handbook, Springer.
[48] National Institute of Standards and Technology, U.S. Department of Commerce (NIST), 2016. http://physics.nist.gov/PhysRefData/XrayMassCoef/tab3.html

NOMENCLATURE

n	Neutron
w	Mass fraction
B	Build-up factor
Cf	Californium 252
E	Energy
I	Intensity
M	mass
S	Source

i) Greek letters

μ	linear attenuation coefficient
γ	gamma ray
ρ	density

ii) Subscript

0	uncollided

iii) Superscript

s	scattered (collided)